

Secondary Periodicity in the Tetrahalogeno Complexes of the Group 13 Elements

Kinga Frąckiewicz,^[a] Marian Czerwiński,^[b] and Sławomir Siekierski*^[a]

Keywords: Quantum calculations / Electronic structure / Group 13 elements / Halogeno complexes / Secondary periodicity

The M–X distances, the charges on the M and X atoms and the natural electron configurations in the hypothetical MX₄[−] molecules, where M is a group 13 element and X = F, Cl, Br, I, have been investigated by quantum calculations. The computed distances are compared with the experimental data, mostly in the Bu₄N[MX₄] salts. We found that: (1) down group 13 both the experimental and calculated M–X distances, the charge on the M atom and the sum of the populations of the M valence orbitals show zigzag variations produced by the filled 3d and 4f shells and by the relativistic effects in the 6s and 6p_{1/2} orbitals; (2) the experimental distances are shorter than the calculated values due, at least in part, to libration of the MX₄[−] anions in the salts; (3) both the

charge on M and the sum of the populations of M valence orbitals point to a highly covalent character of the B–X bonds (except for the B–F bond) and much less covalent character of the M–X bonds formed by the heavier members of the group. In the Al–Tl range the covalent character of the M–X bonds oscillates, and it strongly decreases on passing from the MCl₄[−] to MF₄[−] complexes; (4) the M–X distances (X = Cl, Br, I) are close to the sum of the respective covalent radii, whereas the M–F distances are significantly shorter because of considerable admixture of ionic bonding.

(© Wiley-VCH Verlag GmbH & Co. KGaA, 69451 Weinheim, Germany, 2005)

Introduction

It has been known for a long time that changes in some chemical properties are not uniform down the groups of p-block elements. For instance, despite the general trend of decreasing stability of the highest oxidation state AsCl₅ is, in contrast to SbCl₅, highly unstable,^[1] HBrO₄ shows unexpectedly strong oxidizing properties and BrF₇ is, in contrast to IF₇, not known. These and other non-uniform changes in chemical properties, termed secondary periodicity or zigzag behaviour by Biron,^[2] result from changes in the valence orbitals. Figure 1 shows for the group 13 elements that the *ns* and *np* orbital radii and the covalent radius do not increase uniformly down the group but show an oscillatory, saw-tooth or zigzag variation. The orbital radii shown in Figure 1 are those calculated by Desclaux^[3] and the covalent radii were taken from the literature.^[4] It has been proposed by several authors^[5] that the zigzag changes in orbital radii, energies and ionisation potentials of p-block elements result from incomplete shielding of the nuclear charge for valence electrons by the filled 3d shell (the first anomaly at row 4) and by the filled 4f shell (the second anomaly at row 6). Relativistic effects, which for the 6th row were found to be as important as the lanthanide contraction,^[5b,5c] additionally shift Tl toward In.

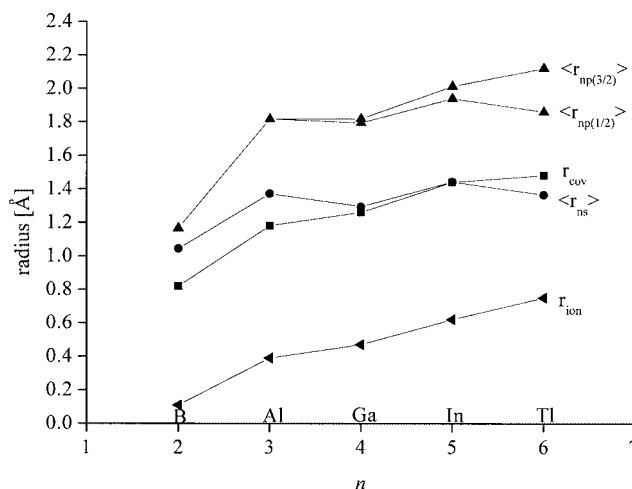


Figure 1. Expectation orbital radii in the atoms, $\langle r_{nl} \rangle$, M³⁺ ionic radius, r_{ion} (CN = 4), and covalent radius, r_{cov} , for the group 13 elements.

The zigzag changes in the radii of valence orbitals should be more or less reproduced by changes in interatomic distances in compounds formed by the p-block elements. Therefore, one can expect a significant increase in the M–X interatomic distance for the group 13 elements when Al is substituted for B, a decrease or small increase in M–X between Al and Ga, a relatively large increase between Ga and In and again a decrease or small increase between In and Tl. However, such a pattern of changes would only be

[a] Institute of Nuclear Chemistry and Technology,
Dorodna 16, 03-195 Warsaw, Poland
E-mail: ssf@ichtj.waw.pl

[b] Jan Długosz University,
Al. Armii Krajowej 13/15, 42-200 Częstochowa, Poland.

observed provided the M–X bonds are essentially covalent. That is because the ionic radius, r_{ion} (CN = 4), in contrast to the covalent radius, r_{cov} , shows only a rudimentary zigzag behaviour (see Figure 1).

The experimental M–H, M–C and M–Cl distances in the MX_k molecules formed by the elements of groups 13–17 have been compiled and discussed by Haaland.^[6] In the above formula the subscript k is equal to one for group 17, two for group 16, three for groups 13 and 15 and four for group 14. The reported distances indeed show zigzag changes, which become less and less conspicuous as one moves from group 13 to group 17, and which seem to be independent of the X atom. The only experimental data which cover all elements of group 13 are those for the M–C bonds in the $\text{M}(\text{CH}_3)_3$ molecules.^[6] These data show a large, very small, relatively large and again a small increase in the M–C distance within the B–Al, Al–Ga, Ga–In and In–Tl pairs, respectively (see Figure 2). Apart from experimental studies on the M–C bond length, the M–X distances in MH, MH_3 , MF and MF_3 molecules formed by the group 13 elements have been computed by Schwerdtfeger et al.^[7] The computed distances in the MH_3 and MF_3 (also in MH and MF) molecules repeat quite well the zigzag variation found experimentally for the M–C distances (Figure 2). However, in contrast to the M–H and M–C bonds, the M–F bond length in MF_3 (also in MF) increases significantly between Al and Ga (see Figure 2), which may be due to a more ionic character of the M–F bond. That the M–F bond is distinctly more ionic than the M–H bond is shown by the metal charge, q_m , which in TlF_3 is almost twice as large as that in TlH_3 .^[7] Up to now, variation in the M–X distances down the groups of p-block elements has been studied only for uncharged molecules. Therefore, it was interesting to find out whether the M–X distances in the MX_4^- ions, where M is a group 13 element and X = F, Cl, Br, I, also show a distinct zigzag variation. One could presume that in the MX_4^- ions the negative charge and the coordination

number four would confer considerable ionic character on the M–X bond. This would make the M–X distance depend more on the ionic radius than on the radii of the outermost s and p orbitals. If so, the M–X distance, like r_{ion} , would show only a feeble zigzag variation (see Figure 1). Moreover, one can also presume that this variation would be more distinct for the MI_4^- , MBr_4^- and MCl_4^- than for the MF_4^- complexes. This is because calculations show that the metal charge, q_m , is 0.67 in TlI_3 (TlI_3 is the hypothetical D_{3h} molecule), 1.08 in TlBr_3 , 1.06 in TlCl_3 and 2.03 in MF_4^- ,^[7] and lower metal charge means less ionic character of the M–X bond. One can expect a similar or even more conspicuous dependence of q_m on X in the MX_4^- ions. In order to check these presumptions we have carried out calculations on the hypothetical gaseous MX_4^- molecules (M = B, Al, Ga, In, Tl and X = F, Cl, Br, I) and compared the calculated M–X distances with the experimental data, mostly in the tetrabutylammonium salts of the MX_4^- anions.

Results and Discussion

M–X Bond Lengths

The experimental M–X distances in the MX_4^- complexes and the computed distances in the hypothetical gaseous MX_4^- molecules (X = F, Cl, Br, I) formed by the group 13 elements are shown in Table 1 and Figure 3. The experimental M–X distances in the tetrabutylammonium salts of AlBr_4^- , GaX_4^- (X = Cl, Br, I), InI_4^- and TlX_4^- (X = Cl, Br) are those reported in our previous papers.^[8–10] The Al–I, In–X (X = Cl, Br) and Tl–I distances in the tetrabutylammonium salts were taken from other papers.^[11–13] Since we have found no data on the $\text{Bu}_4\text{N}[\text{BX}_4]$ and $\text{Bu}_4\text{N}[\text{AlCl}_4]$ salts, the B–Cl and the Al–Cl distances are those in $\text{HP}(2\text{-methylphenyl})_3[\text{BCl}_4]$ ^[14] and $\text{H}_2\text{PMe}_2[\text{AlCl}_4]$.^[15] The B–F distance is the average of the distances in $\text{Me}_4\text{N}[\text{BF}_4]$,^[16] $\text{Me}_3\text{PhN}[\text{BF}_4]$ ^[17] and $\text{Pr}_4\text{N}[\text{BF}_4]$.^[18] whereas the Al–F distance is that in $\text{Ph}_4\text{P}[\text{AlF}_4]$.^[19] Comparison of the average Tl–Cl distance in the tetramethylammonium salt^[8] with that in the tetrabutylammonium salt^[20] (2.416 Å and 2.393 Å, respectively) and of the Al–Cl distance in the Li– AlCl_4 and Cs– AlCl_4 salts^[21] (2.137 Å and 2.119 Å) shows that the effect of the cation on the M–X distance is within about 0.02 Å. This makes it possible to study the secondary periodicity in the M–X distance using the data from MX_4^- salts of different cations. We have also found no experimental data on the B–X distances in the BX_4^- complexes (X = Br, I) and we failed to synthesise the corresponding tetrabutylammonium salts. However, comparison of the data for the $\text{Bu}_4\text{N}[\text{MX}_4]$ salts shows that in the Al–Tl range the differences in the distances $|\text{M–Br}| - |\text{M–Cl}|$ and $|\text{M–I}| - |\text{M–Cl}|$, are independent of M within about 0.015 Å. This allowed us to estimate the B–Br and B–I distances from the experimental B–Cl distance. Since each MX_4^- anion in the $\text{Bu}_4\text{N}[\text{MX}_4]$ salts is surrounded by five Bu_4N^+ cations, which form a highly distorted trigonal bipyramid, the anions are also distorted and show either two pairs of M–

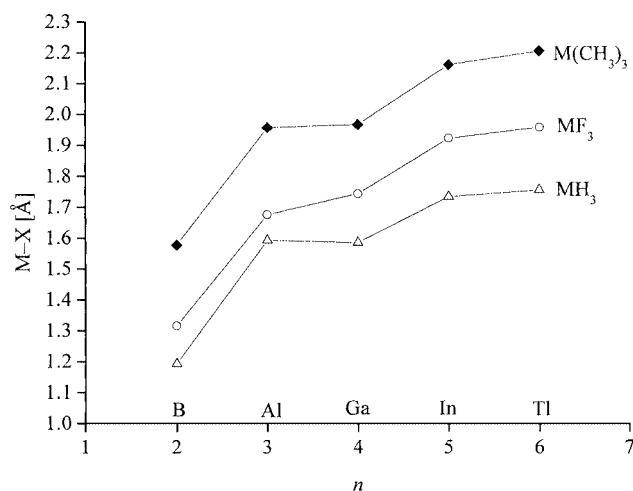


Figure 2. Experimental M–C^[6] and calculated M–H and M–F^[7] distances in the $\text{M}(\text{CH}_3)_3$, MH_3 and MF_3 molecules formed by the group 13 elements.

X distances (orthorhombic system) or four different M–X distances (monoclinic system),^[8] with the difference between the longest and shortest M–X distance being about 0.015 Å. In the salts of cations other than the Bu_4N^+ cation the MX_4^- tetrahedra are also distorted. Therefore, the experimental M–X distances collected in Table 1 and the experimental distances in Figures 3, 6 and 7 are average values. Since the hypothetical gaseous tetrahedral MX_4^- molecules are free from any external influence they show only one M–X distance.

Table 1. Experimental and calculated M–X distances [Å] in the MX_4^- complexes.

	M–F		M–Cl		M–Br		M–I	
	exp.	calcd.	exp.	calcd.	exp.	calcd.	exp.	calcd.
B	1.346	1.410	1.856	1.868	1.99 ^[a]	2.037	2.23 ^[a]	2.271
Al	1.647	1.720	2.127	2.166	2.27	2.336	2.522	2.574
Ga		1.822	2.169	2.233	2.307	2.389	2.545	2.617
In		1.966	2.350	2.375	2.479	2.531	2.702	2.758
Tl		2.021	2.393	2.443	2.534	2.606	2.759	2.825

[a] Estimated.

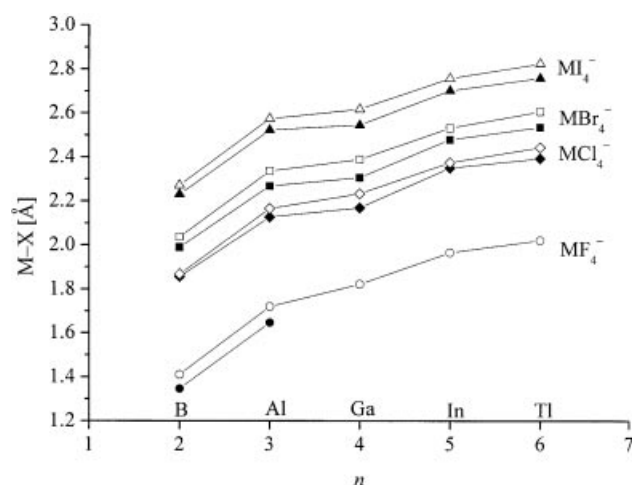


Figure 3. Experimental (filled symbols) and calculated (open symbols) M–X distances in the MX_4^- anions formed by the group 13 elements ($\text{X} = \text{F}, \text{Cl}, \text{Br}, \text{I}$).

It follows from the data in Table 1 and Figure 3 that the M–X distances calculated by the MP2/MBW method with the 2d polarisation function are longer than the experimental distances by about 0.05 Å on average. The B–X, Al–X and Ga–X distances ($\text{X} = \text{F}, \text{Cl}, \text{Br}$) calculated by the MP2/6-311+G* method and the M–Cl distance ($\text{M} = \text{Al}, \text{Ga}, \text{In}, \text{Tl}$) calculated by the MP2/MBW method with the 2s/2p/1d basis set are also longer than the experimental value by about 0.04 Å. Irrespective of the method, the biggest differences for each X are observed for gallium and thallium. This is because large-core pseudopotential calculations without including core-polarisation effects overestimate the Ga–X and Tl–X distances in particular. Three major factors may be responsible for the difference between the experimental and calculated M–X distances. The first is libration of the MX_4^- anion in the salt, which makes the experimental M–X distance shorter than that in the free

MX_4^- molecule^[22] that is the subject of the calculations. The second factor is electrostatic interaction in the salt between the MX_4^- anion and the “infinite” number of consecutive coordination shells containing alternately the Bu_4N^+ cations and the MX_4^- anions. This interaction may either expand or shrink the MX_4^- anion, depending on the number of cations and anions in each shell and on the shell radius. Obviously, the first shell, which contains cations, increases the M–X distance because there is a positive charge on the M atom and a negative charge on the X atom. The following shells alternately decrease and increase the M–X distance. However, because of the complex geometry of the system and the great number of shells that must be taken into account, calculation of the final outcome is unfeasible. The third factor may be a systematic error in the M–X distances calculated by the MP2/MBW method. Indeed, a comparison of calculated^[7] and experimental^[23] distances in the gaseous MH and MF molecules, where $\text{M} = \text{B}, \text{Al}$ and In , shows that the calculated distances are longer than the experimental by about 0.015 Å on average. However, it is important to note that both the experimental and computed distances show a similar zigzag variation down the group, although it is slightly less conspicuous in the calculated distances. This is because, as pointed out above, calculations overestimate the Ga–X and Tl–X distances in particular. In the range from Cl to I the zigzag variation in the M–X bond length seems to be almost independent of the halogen atom and resembles that observed for the MH_3 , $\text{M}(\text{CH}_3)_3$ and MF_3 molecules, (see Figure 2). This similarity shows that the electronegativity of the ligand atom, the number of ligands and the charge on the molecule do not substantially affect the zigzag variation in the M–X distances. However, more detailed examination of changes in the calculated M–X distances (see Table 1 and Figure 3) shows that the zigzag variation in MF_4^- is less conspicuous than in the remaining MX_4^- molecules, which suggests a more ionic character of the M–F bond.

Charges on the Atoms and Natural Electron Configurations

Table 2 shows the calculated atomic charges on the M and X atoms in the MX_4^- molecules, and Figure 4 is a plot of the charge on the metal atom as a function of the row number. The atomic charges were calculated using the B3LYP method with the LANL2DZ basis set. The charge on M and the charge on X, the latter multiplied by four, add almost exactly to –1. Figure 4 shows that the charge on the metal atom, q_m , in each complex increases strongly between B and Al, whereas in the range from Al to Tl it only shows large oscillations. Except for the $\text{BCl}_4^-/\text{BBr}_4^-$ pair, q_m increases when Br is substituted for I, Cl for Br and F for Cl. The increase in q_m between MCl_4^- and MF_4^- is more than twice as large as that between MI_4^- and MCl_4^- , which points to the singular properties of the fluorine complexes. Table 3 shows the natural electron configurations of the M and X atoms in the MX_4^- molecules; the sum of the populations of the s and p valence orbitals in

the M atoms, calculated from the electron configurations, is plotted as a function of the row number in Figure 5. Except for boron, the $(n+1)s$ orbitals are practically not occupied and the population of the $(n+1)p$ orbitals is, on average, smaller than 0.03. It is important to note that both q_m and the sum of populations (the latter reflected in the x -axis) show a zigzag variation similar to that in the M–X distance, although it is much more conspicuous. Since both the low value of q_m and the high population of the valence orbitals of the metal atom mean more covalent character of the M–X bonds we conclude that: (1) the B–X bonds are highly covalent, except for the B–F bond, which is significantly less covalent; (2) bonding becomes much less covalent in the Al–Tl range, where the bond character shows strong oscillations. These oscillations are generated by the filled 3d shell (bonding becomes more covalent for Ga than for Al) and by the joint effect of the filled 4f shell and relativistic effects in the 6s and $6p_{1/2}$ orbitals (bonding becomes more covalent for Tl than for In); (3) for each M bonding becomes less covalent on passing from the MI_4^- to MCl_4^- complexes and much less covalent on passing from the MCl_4^- to MF_4^- complexes.

Table 2. Charges on the M (q_m) and X (q_x) atoms in the MX_4^- molecules.

	MF_4^-		MCl_4^-		MBr_4^-		MI_4^-	
	q_m	q_x	q_m	q_x	q_m	q_x	q_m	q_x
B	0.413	−0.353	−0.238	−0.191	−0.154	−0.211	−0.400	−0.150
Al	1.621	−0.655	0.842	−0.460	0.730	−0.432	0.504	−0.376
Ga	1.494	−0.624	0.701	−0.425	0.569	−0.392	0.346	−0.336
In	1.629	−0.657	0.885	−0.471	0.733	−0.433	0.518	−0.379
Tl	1.502	−0.626	0.845	−0.461	0.716	−0.429	0.544	−0.386

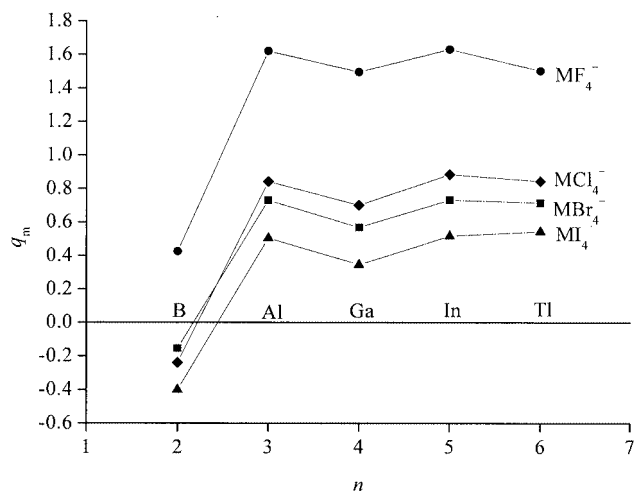


Figure 4. The charge on the group 13 metal atom, q_m , in the MF_4^- , MCl_4^- , MBr_4^- and MI_4^- molecules.

Correlation Between the M–X Distance and the Covalent Radius

Since in the Al–Tl range the ionic radius, r_{ion} (CN = 4), shows only a weak zigzag variation (see Figure 1), one can-

Table 3. Natural electron configurations of the M and X atoms in the MX_4^- molecules.

	MF_4^-		MCl_4^-		MBr_4^-		MI_4^-	
B	2s ^{0.41}	2p ^{1.19}	B	2s ^{0.78}	2p ^{1.85}	B	2s ^{0.92}	2p ^{2.09}
F	3s ^{1.89}	3p ^{5.69}	Cl	3s ^{1.83}	3p ^{5.49}	Br	4s ^{1.82}	4p ^{5.40}
Al	3s ^{0.32}	3p ^{0.57}	Al	3s ^{0.60}	3p ^{1.07}	Al	3s ^{0.71}	3p ^{1.24}
F	3s ^{1.94}	3p ^{5.82}	Cl	3s ^{1.90}	3p ^{5.68}	Br	4s ^{1.88}	4p ^{5.62}
Ga	4s ^{0.41}	4p ^{0.57}	Ga	4s ^{0.74}	4p ^{1.03}	Ga	4s ^{0.86}	4p ^{1.20}
F	3s ^{1.95}	3p ^{5.80}	Cl	3s ^{1.91}	3p ^{5.64}	Br	4s ^{1.89}	4p ^{5.58}
In	5s ^{0.40}	5p ^{0.49}	In	5s ^{0.69}	5p ^{0.90}	In	5s ^{0.80}	5p ^{1.02}
F	3s ^{1.96}	3p ^{5.81}	Cl	3s ^{1.93}	3p ^{5.67}	Br	4s ^{1.92}	4p ^{5.62}
Tl	6s ^{0.55}	6p ^{0.43}	Tl	6s ^{0.89}	6p ^{0.75}	Tl	6s ^{1.01}	6p ^{0.84}
F	3s ^{1.97}	3p ^{5.78}	Cl	3s ^{1.94}	3p ^{5.65}	Br	4s ^{1.93}	4p ^{5.60}
						I	5s ^{1.92}	5p ^{5.54}

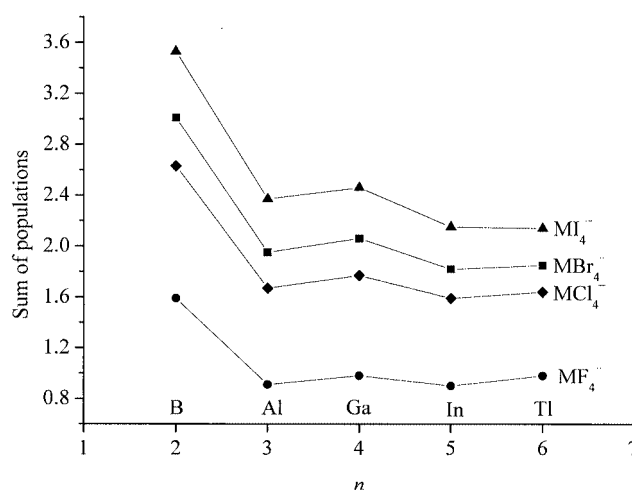


Figure 5. The sum of the populations of metal s and p valence orbitals in the MF_4^- , MCl_4^- , MBr_4^- and MI_4^- molecules of the group 13 elements.

not expect the experimental M–X distance to depend linearly on r_{ion} , as documented in Figure 6. On the other hand, a comparison of the data in Figures 1 and 4 shows that the covalent radius and the average M–X distance in the MX_4^- ions change in a very similar way down group 13, so that a linear correlation between the two can be expected. Figure 7 shows the experimental M–X distance in the MX_4^- complexes as a function of the sum of the covalent radii of the M and X atoms [$r_{cov}(M) + r_{cov}(X)$]. We can see from Figure 7 that for X = Cl, Br, I the experimental M–X distance depends linearly on the sum of the covalent radii. Moreover, the M–X distance is very close to the sum of the respective covalent radii. On the other hand, the experimental B–F and Al–F distances suggest a separate downward-shifted linear plot for the MF_4^- complexes. In order to show that all M–F distances form a separate lower-lying linear branch we have additionally plotted the calculated M–F distances in Figure 7. Since these are greater than the experimental values (as are the calculated M–Cl, M–Br and M–I distances), their position clearly shows that all experimental M–F distances would form a separate

lower-lying branch. It is worthy to note that the M–C and M–H distances in the $M(\text{CH}_3)_3$ and $M\text{H}_3$ molecules^[6,7] also form a common linear plot, with the M–X distance close to the sum of the respective covalent radii, whereas the M–F distances in the MF_3 molecules^[7] belong to a separate lower-lying branch (see Figure 8). That the length of the M–F bond is considerably shorter than that expected from the sum of the covalent radii results from a significant admixture of ionic bonding. Using somewhat outdated but visual language, one can say that the decrease in the M–F bond length results from the resonance between the covalent and ionic structures.

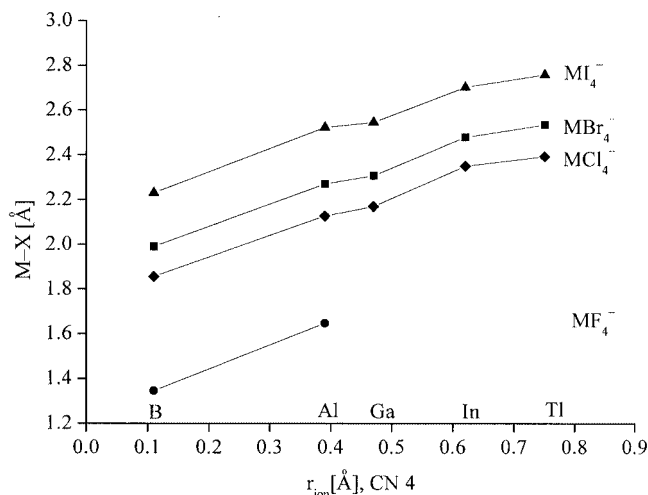


Figure 6. The experimental M–X distance in the MX_4^- anions as a function of the ionic radius, r_{ion} (CN = 4). M is a group 13 element and X = F, Cl, Br, I.

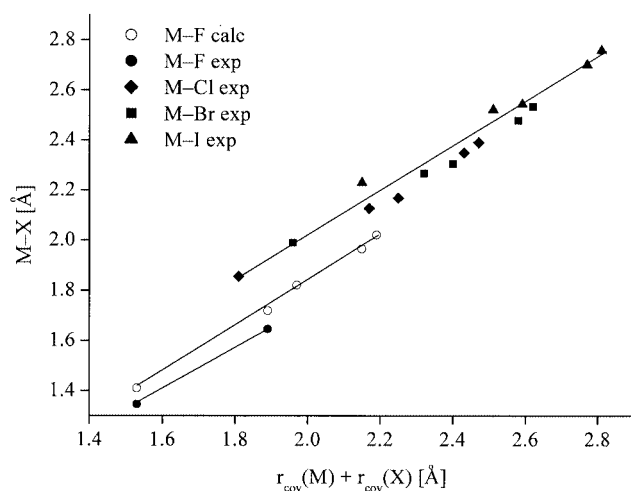


Figure 7. Experimental and calculated M–X distances in the MX_4^- molecules as a function of the sum of the covalent radii $[r_{\text{cov}}(\text{M}) + r_{\text{cov}}(\text{X})]$. M is a group 13 element and X = F, Cl, Br, I.

Changes in the Unit Cell Volumes

The $\text{Bu}_4\text{N}[\text{MX}_4]$ salts of the group 13 elements studied till now crystallise for each M either in the $Pnma$ (X = Cl,

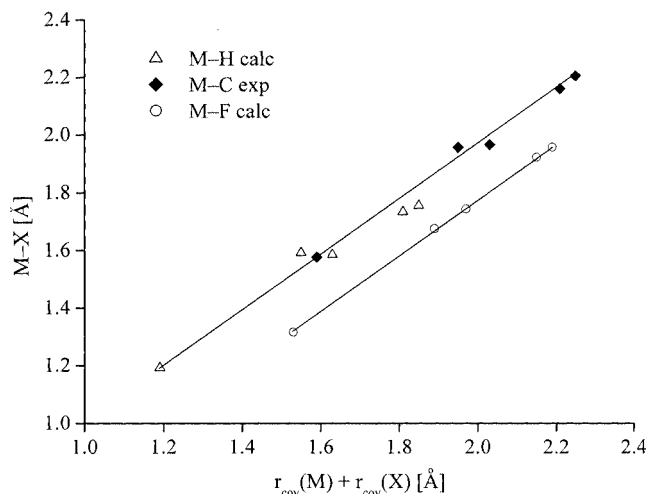


Figure 8. Experimental and calculated M–X distances in the MX_3 molecules^[6,7] as a function of the sum of the covalent radii $[r_{\text{cov}}(\text{M}) + r_{\text{cov}}(\text{X})]$. M is a group 13 element and X = H, C, F.

Br) or in the $P2_1/n$ (X = I) space groups.^[8] Therefore, for a given X the zigzag variation in the M–X distance, i.e. in the volume of the MX_4^- anion, results in a similar variation in the unit cell volume (Figure 9). Because of the interaction between the MX_4^- anion and the five Bu_4N^+ cations from the nearest coordination shell, the zigzag variation in the volume of the anion generates zigzag variation in the anion-to-cation distance, i.e. in the M–N distance. For example, according to the data for the $\text{Bu}_4\text{N}[\text{MI}_4]$ salts,^[8] the average M–N distance is equal to 6.584, 6.581, 6.630 and 6.622 Å, for Al, Ga, In and Tl, respectively. Since there is a decrease, an increase and again a decrease in the M–N distance for the consecutive pairs of elements, these data indeed show a distinct zigzag variation in the M–N distance. However, it should be noticed that the overall increase in the M–X distance in the $\text{Bu}_4\text{N}[\text{MX}_4]$ salts between Al and Tl is equal to 0.237 Å, whereas the respective increase in the M–N distance is equal to only 0.037 Å. This is because the X atoms are located near the end-atoms of the butyl chains, where

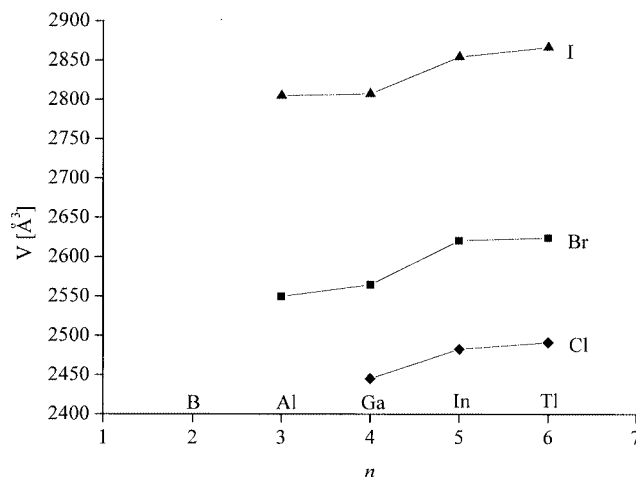


Figure 9. Unit cell volumes of the $\text{Bu}_4\text{N}[\text{MX}_4]$ salts as a function of the row number. M is a group 13 element and X = Cl, Br, I.

there is enough space for the X atom to change its position without significantly moving the whole Bu_4N^+ cation.

Conclusions

We can draw the following conclusions from our calculations and from the available experimental data.

(1) In group 13 both the experimental M–X distances in the MX_4^- salts (mainly tetrabutylammonium salts) and the computed M–X distances in the hypothetical gaseous MX_4^- molecules ($\text{X} = \text{F}, \text{Cl}, \text{Br}, \text{I}$) show almost the same zigzag variation down the group, although slightly less conspicuous in the calculated values. This is because large-core pseudopotential calculations without including core-polarisation effects overestimate the Ga–X and Tl–X distances in particular. The variation in both the experimental and calculated bond length in the MX_4^- ions is similar to those in the MH_3 , $\text{M}(\text{CH}_3)_3$, MF_3 , MH and MF molecules. This means that the general pattern of changes in the metal-to-ligand distance down the group 13 is not substantially affected by the electronegativity of the ligand atom, the coordination number of the M atom or the charge on the molecule. However, a comparison of the calculated M–X distances in the MX_4^- molecules shows a less distinct zigzag variation in the M–F distance, which points to a more ionic character of the M–F bonds.

(2) The experimental M–X distances are shorter (on average by about 0.05 Å) than the calculated values. The main reason seems to be libration of the MX_4^- anions in the salts, which is absent in the hypothetical gaseous MX_4^- molecules. Moreover, the MP2/MBW method may slightly overestimate the calculated M–X distances. On the other hand, interaction of the MX_4^- anion with a large number of the coordination shells containing alternately cations and anions may either increase or decrease the experimental M–X distance, i.e. either decrease or increase the difference between the calculated and experimental M–X distances. However, the final outcome for many shells is difficult to calculate.

(3) Both the charge on the M atom, q_m , and the sum of the populations of M valence orbitals show very distinct zigzag variations down group 13, which points to the highly covalent character of the M–X bond formed by boron (except for the B–F bond) and distinctly less covalent for the heavier members of the group. The bond character oscillates strongly in the range from Al to Tl due to the filled 3d shell and to the joint effect of the filled 4f shell and relativistic effects in the 6s and $6p_{1/2}$ orbitals. The covalent character of the bond decreases between the MI_4^- and MCl_4^- complexes for all the group 13 elements and decreases significantly on passing from the MCl_4^- to MF_4^- complexes.

(4) The M–X bond length ($\text{X} = \text{Cl}, \text{Br}, \text{I}$) is close to the sum of the covalent radii. The much greater ionic character of the M–F bond, documented by the high value of q_m , low population of metal valence orbitals and less-conspicuous zigzag variation in the calculated M–F distances, makes the M–F bond length significantly shorter than the sum of the covalent radii.

(5) The M–X distances in the simple MX_k molecules ($\text{X} = \text{H}, \text{CH}_3, \text{Cl}$) formed by the group 14–17 elements show a zigzag variation^[6] down each group similar to that in the MX_4^- complexes discussed in this paper. Since we have shown that the zigzag variation in the M–X distance for the MX_4^- complexes correlates with changes in the charge on the central atom and with changes in the population of its valence orbitals, we presume that the contribution from covalent bonding in the MX_k molecules of groups 14–17 changes in a way similar to that found for the MX_4^- complexes of the group 13 elements.

Calculations

In quantum calculations we used the nonrelativistic Hartree–Fock (NRHF) method^[24] as well as the Kohn–Sham Density Functional Theory (DFT),^[25] and methods which take into account relativistic effects through the use of a relativistic effective core potential (RECP). Calculations carried out in the frame of the NRHF method include electron correlation by Møller–Plesset (MP2)^[26] for the 6-311+G* basis set.^[27] To take into account relativistic effects we used the Stuttgart/Dresden basis sets and pseudopotentials adjusted to Wood–Boring data (MBW).^[28] In the DFT method we chose a hybrid potential of the type B3LYP^[29] and carried out calculations for all atoms using the LANL2DZ basis set.^[30] Additionally, for all elements we introduced two polarisation functions of the d type whose orbital exponents are given by Huzinaga.^[31] In the frame of the methods with pseudopotential we assumed that electrons in the closed shells enter into the core, thereby designating its effective potential. Using the MP2/MBW method with the 2d polarisation function we determined the global optimum geometry with regard to distances and angles for all the MX_4^- molecules, where $\text{M} = \text{B}, \text{Al}, \text{Ga}, \text{In}, \text{Tl}$ and $\text{X} = \text{F}, \text{Cl}, \text{Br}, \text{I}$. In order to compare the geometries obtained in this way we carried out calculations using the MP2/6-311+G* method with the basis set which takes into account polarisation and dispersive effects to the greatest possible extent. Because of problems with availability of the 6-311+G* basis sets for heavier atoms, the optimum geometry in this method could only be obtained for the MX_4^- molecules, where $\text{M} = \text{B}, \text{Al}, \text{Ga}$ and $\text{X} = \text{F}, \text{Cl}, \text{Br}$. For $\text{M} = \text{B}, \text{Al}, \text{Ga}, \text{In}, \text{Tl}$ and $\text{X} = \text{Cl}$ we also carried out calculations using the MP2/MBW method and the Stuttgart/Dresden basis sets complemented by the 2s/2p/1d set with one polarisation function of the d type, for which the orbital exponent is given by Huzinaga.^[31] Using this method we obtained somewhat better agreement between the calculated and experimental distances in comparison with those obtained by the MP2/MBW method with the 2d polarisation function. However, because of problems with availability of the basis sets we were only able to carry out calculations for the MCl_4^- molecules. For the optimised geometry we calculated the charges on the atoms in the studied molecules by the B3LYP/LANL2DZ method. This method, in contrast to the MP2/MBW method, gives charges on the atoms, which are compatible with changes in the M–X distance and in the occupation of metal valence orbitals. We determined the natural electron configurations of the M and X atoms based on the procedure of natural orbital analysis.^[32] The calculations were carried out with the Gaussian 98 package.^[33]

[1] a) K. Seppelt, *Z. Anorg. Allg. Chem.* **1977**, 434, 5–15; b) S. Haupt, K. Seppelt, *Z. Anorg. Allg. Chem.* **2002**, 628, 729–734.

[2] E. V. Biron, *Zh. Russk. Fiz.-Kim. Obshch.* **1915**, 47, 964–988.

[3] J. P. Desclaux, *At. Data Nucl. Data Tables* **1973**, 12, 311–406.

- [4] C. H. Suresh, N. Koga, *J. Phys. Chem. A* **2001**, *105*, 5940–5944.
- [5] a) N. N. Greenwood, K. J. Wade, *J. Chem. Soc.* **1956**, 1527–1536; b) P. Pyykkö, *J. Chem. Res.* **1979**, *12*, 380–381; c) P. S. Bagus, Y. S. Lee, K. S. Pitzer, *Chem. Phys. Lett.* **1975**, *33*, 408–411; d) P. Pyykkö, *Chem. Rev.* **1988**, *88*, 563–595.
- [6] A. Haaland, *J. Mol. Struct.* **1988**, *97*, 115–128.
- [7] P. Schwerdtfeger, G. A. Heath, M. Dolg, M. A. Bennet, *J. Am. Chem. Soc.* **1992**, *114*, 7518–7527.
- [8] K. Rudawska-Frąckiewicz, S. Siekierski, *J. Coord. Chem.* **2004**, *57*, 777–784.
- [9] K. Rudawska, H. Ptasiwicz-Bąk, *J. Coord. Chem.* **2003**, *56*, 1567–1574.
- [10] K. Rudawska, H. Ptasiwicz-Bąk, S. Siekierski, *J. Coord. Chem.* **2002**, *55*, 403–409.
- [11] R. D. Rogers, J. C. Backer, J. L. Atwood, *J. Cryst. Spect. Res.* **1984**, *14*, 333–339.
- [12] M. A. Khan, D. G. Tuck, *Acta Crystallogr., Sect. B* **1982**, *38*, 803–806.
- [13] a) J. Glaser, P. L. Gogin, M. Sandström, V. Lustko, *Acta Chem. Scand. A* **1982**, *36*, 55–62; b) J. Glaser, P. L. Gogin, M. Sandström, V. Lustko, *Acta Chem. Scand. A* **1982**, *37*, 437–438.
- [14] J. M. Burke, J. A. K. Howard, T. B. Marder, C. Wilson, *Acta Crystallogr., Sect. C* **2000**, *56*, 1354–1355.
- [15] Ch. Aubauer, K. Davidge, T. M. Klapötke, P. Mayer, *Z. Anorg. Allg. Chem.* **2000**, *626*, 1783–1786.
- [16] G. Giuseppetti, F. Mazzi, C. Tadini, *Z. Kristallogr.* **1992**, *202*, 81–88.
- [17] Th. Wiest, H. Eickmeier, H. Reuter, R. Blachnik, *Z. Kristallogr.* **2000**, *215*, 52–55.
- [18] G. Giuseppetti, F. Mazzi, C. Tadini, P. Ferloni, G. Zabinska, S. Torre, *Z. Kristallogr.* **1997**, *212*, 367–371.
- [19] M. Ferbinteanu, H. W. Roesky, F. Cimpoesu, M. Atanasov, S. Köpke, R. Herbst-Irmer, *Inorg. Chem.* **2001**, *40*, 4947–4955.
- [20] M. Lenck, S.-Q. Dou, A. Weiss, *Z. Naturforsch., Teil A* **1991**, *46*, 777–784.
- [21] G. Mairesse, P. Barbier, J. P. Wignacourt, *Acta Crystallogr., Sect. B* **1979**, *35*, 1573–1580.
- [22] Y. Ishii, T. Terao, S. Hayashi, *J. Chem. Phys.* **1997**, *107*, 2760–2774.
- [23] “Tables of Interatomic Distances and Configurations”, in *Molecules and Ions*, The Chemical Society, London, **1958**.
- [24] C. C. J. Roothan, *Rev. Mod. Phys.* **1951**, *23*, 69–89.
- [25] a) P. Hohenberg, W. Kohn, *Phys. Rev. B* **1964**, *136*, 864–871; b) W. Kohn, L. J. Sham, *Phys. Rev. A* **1965**, *140*, 1133–1138; c) R. G. Parr, W. Yang, *Density-Functional Theory of Atoms and Molecules*, Oxford University Press, Oxford, **1989**.
- [26] a) M. Head-Gordon, J. A. Pople, M. J. Frisch, *Chem. Phys. Lett.* **1988**, *153*, 503–506; b) M. J. Frisch, M. Head-Gordon, J. A. Pople, *Chem. Phys. Lett.* **1990**, *166*, 275–280; c) M. J. Frisch, M. Head-Gordon, J. A. Pople, *Chem. Phys. Lett.* **1990**, *166*, 281–289; d) M. Head-Gordon, T. Head-Gordon, *Chem. Phys. Lett.* **1994**, *220*, 122–128; e) S. Saebo, J. Almlof, *Chem. Phys. Lett.* **1989**, *154*, 83–89.
- [27] L. A. Curtiss, M. P. McGrath, J. P. Blaudeau, N. E. Davis, R. C. Binning, Jr., L. Radom, *J. Chem. Phys.* **1995**, *103*, 6104–6113.
- [28] T. Leininger, A. Nicklass, H. Stoll, M. Dolg, P. Schwerdtfeger, *J. Chem. Phys.* **1996**, *105*, 1052–1059.
- [29] C. Lee, W. Yang, R. G. Parr, *Phys. Rev. B* **1988**, *37*, 785–789.
- [30] a) T. H. Dunning, Jr., P. J. Hay, in *Modern Theoretical Chemistry* (Ed.: H. F. Schaefer, III), Plenum, New York, **1976**; b) P. J. Hay, W. R. Wadt, *J. Chem. Phys.* **1985**, *82*, 270–283; c) W. R. Wadt, P. J. Hay, *J. Chem. Phys.* **1985**, *82*, 284–298; d) P. J. Hay, W. R. Wadt, *J. Chem. Phys.* **1985**, *82*, 299–310.
- [31] S. Huzinaga, *Gaussian Basis Sets for Molecular Calculations*, Elsevier, New York, **1984**.
- [32] A. E. Reed, L. A. Curtiss, F. Weinhold, *Chem. Rev.* **1988**, *88*, 899–926.
- [33] M. J. Frisch, G. W. Trucks, H. B. Schlegel, G. E. Scuseria, M. A. Robb, J. R. Cheeseman, V. G. Zakrzewski, J. A. Montgomery, Jr., R. E. Stratmann, J. C. Burant, S. Dapprich, J. M. Millam, A. D. Daniels, K. N. Kudin, M. C. Strain, O. Farkas, J. Tomasi, V. Barone, M. Cossi, R. Cammi, B. Mennucci, C. Pomelli, C. Adamo, S. Clifford, J. Ochterski, G. A. Petersson, P. Y. Ayala, Q. Cui, K. Morokuma, D. K. Malick, A. D. Rabuck, K. Raghavachari, J. B. Foresman, J. Cioslowski, J. V. Ortiz, A. G. Baboul, B. B. Stefanov, G. Liu, A. Liashenko, P. Piskorz, I. Komaromi, R. Gomperts, R. L. Martin, D. J. Fox, T. Keith M. A. Al-Laham, C. Y. Peng, A. Nanayakkara, C. Gonzalez, M. Challacombe, P. M. W. Gill, B. Johnson, W. Chen, M. W. Wong, J. L. Andres, C. Gonzalez, M. Head-Gordon, E. S. Replogle, J. A. Pople, *Gaussian 98*, Revision A.7, Gaussian, Inc., Pittsburgh, PA, **1998**.

Received: March 24, 2005

Published Online: August 29, 2005